

Modelling of PHEMT Low-frequency i/v Characteristics Through a New Large-Signal Measurement Setup

A.Raffo, A.Santarelli, P.A.Traverso, M.Pagani, G.Vannini, F.Filicori

Abstract— Large-signal dynamic modelling of III-V FETs cannot be simply based on DC i/v characteristics when accurate performance prediction is needed. In fact, dispersive phenomena due to self-heating and/or traps (surface state densities and deep level traps) must be taken into account since they cause important deviations in the low-frequency dynamic drain current. Thus, static characteristics should be replaced with a suitable model which also accounts for low-frequency dispersive effects. Different approaches have been proposed by the research community and quite often a characterisation by means of pulsed i/v measurement systems has been suggested as the more appropriate for the identification of low-frequency drain current models. As a possible alternative to relatively expensive, special-purpose pulsed i/v instrumentation, a new large-signal measurement setup, which is based on simple low-frequency sinusoidal excitation easily reproducible with conventional general-purpose instrumentation, is adopted in the paper to extract two different models for the low-frequency dynamic i/v PHEMT characteristics. Experimental results on the prediction of intermodulation distortion are also provided.

Index Terms—Dispersive effects, Intermodulation distortion, Non-linear measurement, Non-linear modelling, PHEMT.

I. THE LARGE-SIGNAL I/V MEASUREMENT SETUP

THE measurement system proposed is shown in Fig.1. The two independent output channels of an arbitrary function generator (with 50Ω output impedance) are used for feeding the DUT with a sinusoidal voltage waveform in the frequency range 2-12 MHz and for triggering a digital sampling oscilloscope, which provides acquisitions of the incident and reflected waves at the

transistor ports. To this aim, an oscilloscope with four input channels, each one sampled up to 4 GSa/s, is used. Moreover, a high resolution (4μV; 20fA) highly accurate (V: 0.05%, I: 0.2%) dc source provides the bias for the DUT. Monitoring of incident and reflected waves at the DUT input is obtained by means of a wide bandwidth (10kHz – 1000MHz) dual directional coupler, while 100kHz–6000MHz bandwidth bias-tees with low insertion loss (0.15dB) are used for suitable dc and rf path isolation and also for ensuring stability. In order to provide different, purely resistive DUT loading conditions, SMD-type resistors having different values were mounted on FR4-substrate boards and "series" wired through 50Ω transmission lines to external SMA connectors (the total loading resistance obtained being the sum of the SMD resistor value and the 50Ω oscilloscope input impedance). Minimum phase rotations are obtained by connecting the selected board as close as possible to the drain probe.

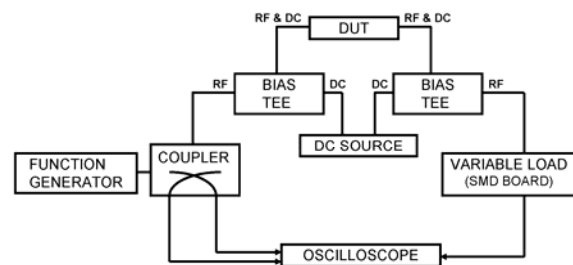


Fig. 1. The proposed large-signal measurement setup.

The simplicity of the setup represents its major advantage, since at the frequency of a few MHz all the system components satisfy linear non-distortion conditions greatly simplifying the needed calibration procedure. To this aim, the setup can be divided into a suitable number of signal paths to be characterized in terms of attenuations and delays in the working frequency range [1].

The accuracy of the described measurement setup has been tested under small-signal conditions. In particular, the dynamic trans-conductance of a 0.25μm Triquint GaAs PHEMT (W=600μm) was measured under small-signal sinusoidal excitation and 50Ω loading conditions by means of a vector network analyzer in the 2-12 MHz frequency range. The obtained results were then compared with the corresponding quantities measured with the proposed measurement setup. The agreement found [1]

This work was partly funded by MIUR (Italian Ministry of Instruction, University and Research) and also performed in the context of the network TARGET – “Top Amplifier Research Groups in a European Team” supported by the Information Society Technologies Program of the EU under contract IST-1-507893-NOE, www.target-net.org.

A. Raffo and G. Vannini are with the Department of Engineering, University of Ferrara, Via Saragat 1, 44100 Ferrara, Italy, e-mail: araffo@ing.unife.it gvannini@ing.unife.it. A. Raffo is also with CoRiTeL, Via Anagnina 203, 00040 Morena (Rome) - Italy.

A. Santarelli, P.A. Traverso and F. Filicori are with the Department of Electronics, University of Bologna, Viale Risorgimento 2, 40136 Bologna, Italy, e-mail: asantarelli@deis.unibo.it, ptraverso@deis.unibo.it, ffilicori@deis.unibo.it.

M. Pagani is with Ericsson Lab Italy S.p.A., Via Cadorna, 73, 20090 Vimodrone (MI), Italy, email: maurizio.pagani@ericsson.com. M. Pagani is also with CoRiTeL, Via Anagnina 203, 00040 Morena (Rome) - Italy.

was always better than 6% .

The ability to measure dc characteristics, small-signal (with comparable accuracy to conventional network analyzers) and large-signal data without modifications in the instrument configuration represents another important advantage of the proposed setup.

Given a generic target $(v_g, v_d)_k$ it can be reached in two different operation modes:

a) the target $(v_g)_k$ corresponds to a minimum of the gate voltage and $(v_d)_k$ to a maximum of the drain voltage waveform;

b) the target $(v_g)_k$ corresponds to a maximum of the gate voltage and $(v_d)_k$ to a minimum of the drain voltage waveform.

Thus two sets of bias voltages V_{g0}, V_{d0} may be found for each k -th dynamic voltage pair $(v_g, v_d)_k$ corresponding respectively to the outlined *a*- and *b*-operation modes. They will be referred to in the following as: A-type and B-type bias. Different values of the dynamic drain current are obtained in these two conditions. In fact, dispersion due to traps and thermal phenomena cause important deviations between static and low frequency dynamic drain current characteristics, which are strongly dependent on quiescent conditions. Definitely, as shown in Fig.2, three different drain current values are obtained from the measurement system for each k -th dynamic voltage pair $(v_g, v_d)_k$: the dc current for $V_{g0}=(v_g)_k, V_{d0}=(v_d)_k$ and the two dynamic values corresponding to the large-signal dynamic operation with the A- and B-type bias.

Finally, the measurement procedure may be repeated for different values of the loading resistor, obtaining a suitably large set of dynamic current measurements for any k -th $(v_g, v_d)_k$ voltage pair.

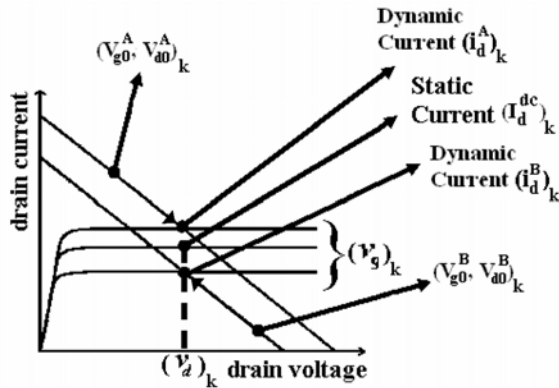


Fig. 2. Three different drain current values, associated with the same $(v_g, v_d)_k$ voltage pair. The middle value corresponds to the dc current; the upper and lower dynamic values are obtained by the large-signal measurement setup using the A-type and B-type bias conditions.

II. LOW-FREQUENCY I/V PHEMT MODELLING

The dynamic drain current measurements obtained with the proposed large-signal setup on a 0.25 μ m Triquant GaAs PHEMT were used for the identification of two different models for the description of low-frequency dispersive phenomena. The first one is a modified version of the look-up-table based Empirical model proposed in

[2]; in particular, a new formulation of the thermal model was adopted here, which allows to replace the equithermal static drain current characteristic as in [2], with the nonequithermal one, directly obtainable from measurements. Moreover, the look-up-table model functions were obtained here by means of a different identification procedure, where minimization of the discrepancies between the predicted and measured dynamic DUT behaviour is carried out under low-frequency small- and large-signal regime instead of under pulsed *i/v* operation as in [2]. Large-signal drain current data were obtained in this case through the proposed measurement setup. Much better conditioning of the model parameters is obtained here with respect to the extraction procedure proposed in [2].

In particular, after theoretical considerations not reported here [3], the drain current can be expressed as:

$$i_d(t) = F^{DC} \{v_g(t), v_d(t)\} + f_g \{v_g(t), v_d(t)\} (v_g(t) - V_{g0}) + f_d \{v_g(t), v_d(t)\} (v_d(t) - V_{d0}) + f_p \{v_g(t), v_d(t)\} (p_s(t) - P_0) \quad (1)$$

where, F^{DC} is the static drain current characteristic, V_{g0}, V_{d0} are the average values of the applied voltages $v_g(t), v_d(t)$, respectively and f_g, f_d, f_p , are three suitable functions to be identified. Moreover, P_0 represents the average dissipated power under dynamic conditions and $p_s(t)$ is a "quasi-static" term [4] corresponding to the power that would be dissipated if $v_g(t), v_d(t)$ were "slowly" time-varying voltages.

Linearization of (1) with respect to $v_g(t)$ and $v_d(t)$ around a generic bias condition (V_{g0}, V_{d0}) leads to:

$$g_m^{AC} \{V_{g0}, V_{d0}\} = g_m^{DC} \{V_{g0}, V_{d0}\} + f_g \{V_{g0}, V_{d0}\} + f_p \{V_{g0}, V_{d0}\} \cdot g_m^{DC} \{V_{g0}, V_{d0}\} \cdot V_{d0} \quad (2)$$

$$g_d^{AC} \{V_{g0}, V_{d0}\} = g_d^{DC} \{V_{g0}, V_{d0}\} + f_d \{V_{g0}, V_{d0}\} + f_p \{V_{g0}, V_{d0}\} \cdot (g_d^{DC} \{V_{g0}, V_{d0}\} \cdot V_{d0} + I_{d0}) \quad (3)$$

where $g_m^{AC}, g_d^{AC}, g_m^{DC}, g_d^{DC}$ represent the trans- and output-conductance under low-frequency (ac) and static (dc) conditions, while I_{d0} is the dc drain current.

For each (v_g, v_d) pair the three model functions f_g, f_d, f_p , were identified by minimizing the squared discrepancies between (1),(2),(3) and corresponding dynamic measures obtained under different operating conditions. In particular, large-signal data obtained through the previously described setup under low-frequency sinusoidal input excitation, and small-signal low-frequency conductances obtained from a conventional VNA were considered here.

A second model of drain current deviations was also identified. This is a Backgating-like model [4], that describes the low frequency dispersive behaviour by

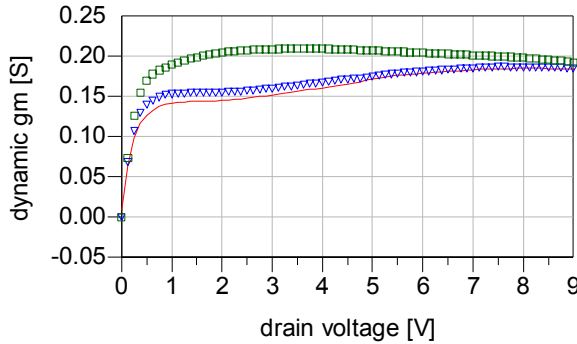
means of a predictive formula based on only three scalar parameters. A modified identification procedure was also used here with respect to [4]. Instead of using only small-signal data, also large-signal current measurements carried out with the proposed system, were used here. In particular, according to [4], the drain current is expressed as:

$$i_d(t) = [1 + K(p_s(t) - P_0)] \cdot F^{DC} \{v_{gx}(t), v_d(t)\} \quad (4)$$

where:

$$v_{gx}(t) = v_g(t) + \alpha_g(v_g(t) - V_{g0}) + \alpha_d(v_d(t) - V_{d0}) \quad (5)$$

Linearization of (4)-(5) with respect to $v_g(t)$ and $v_d(t)$ around a generic bias condition (V_{g0} , V_{d0}) leads to:



$$g_m^{AC} \{V_{g0}, V_{d0}\} = [1 + k \cdot V_{d0} \cdot I_{d0} + \alpha_g] \cdot g_m^{DC} \{V_{g0}, V_{d0}\} \quad (6)$$

$$g_d^{AC} \{V_{g0}, V_{d0}\} = [1 + k \cdot V_{d0} \cdot I_{d0}] \cdot g_d^{DC} \{V_{g0}, V_{d0}\} + k \cdot I_{d0}^2 + \alpha_d \cdot g_m^{DC} \{V_{g0}, V_{d0}\} \quad (7)$$

where α_g , α_d , k are three scalar parameters to be determined, while other terms in (4)-(7) have the same meaning as previously introduced.

Minimization on a suitable grid of bias conditions of the discrepancies between (4)-(7) and corresponding dynamic current/conductance measurements under large- and small signal operation leads to the identification of the three unknown model parameters α_g , α_d , k .

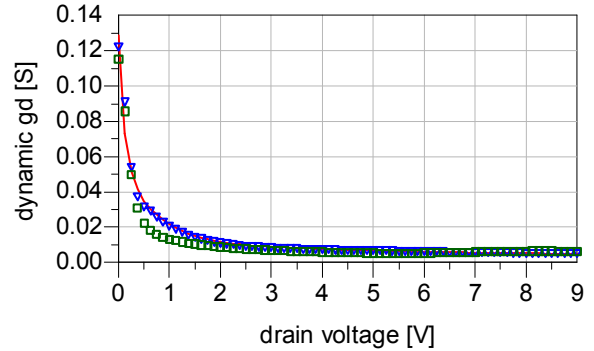


Fig. 3 Trans-conductance (left) and output-conductance (right) of a 0.25 μ m Triquant GaAs PHEMT at different drain biases and $V_{g0} = -0.55$ V ($f = 2$ MHz). Measurements (solid line) versus predictions based on Backgating (squares) and Empirical (triangles) models.

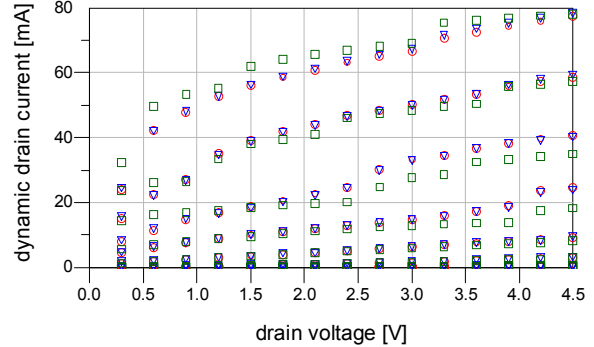
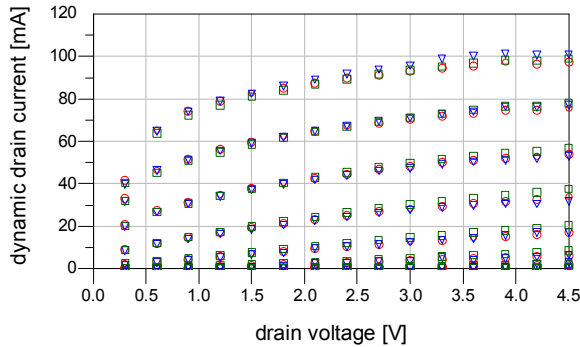


Fig. 4. GaAs 0.25 μ m PHEMT dynamic drain current: measurements (circles) versus predictions based on Backgating (squares) and Empirical (triangles) models for a 320 Ohm load condition and A-type biases (left) and B-type biases (right).

III. EXPERIMENTAL RESULTS

In order to test the small-signal prediction capability of the i/v models, measurements of the PHEMT low-frequency trans- and output-conductance were carried out at different biases above traps cut-off ($f = 2$ MHz) and compared with the Empirical and Backgating model predictions. Corresponding results are shown in Fig.3. As can be seen, predictions are in good agreement with measurements, but as expected and evident, better

prediction accuracy is obtained by means of the look-up-table based empirical model.

Figure 4 shows large-signal drain current measurements carried out with the new measurement setup using 320 Ω resistors and coherent current predictions obtained by means of the Backgating and Empirical i/v models. Also in this context a very good prediction capability of the empirical model can be observed; it must be however outlined the extremely restricted number of model parameters (only three)

adopted in the Backgating model to describe the very complex low frequency dispersive behaviour.

The low-frequency drain current models extracted may be easily embedded in large-signal device models for micro- and millimetre-wave applications, leading to an improvement of their prediction accuracy. In particular, the Empirical and Backgating models were embedded in a non-quasi-static large-signal model, namely the Nonlinear Discrete Convolution (NDC) model presented in [5]. In particular, according to the identification procedure outlined in [5], the NDC model was extracted, for the same Triquint GaAs PHEMT.

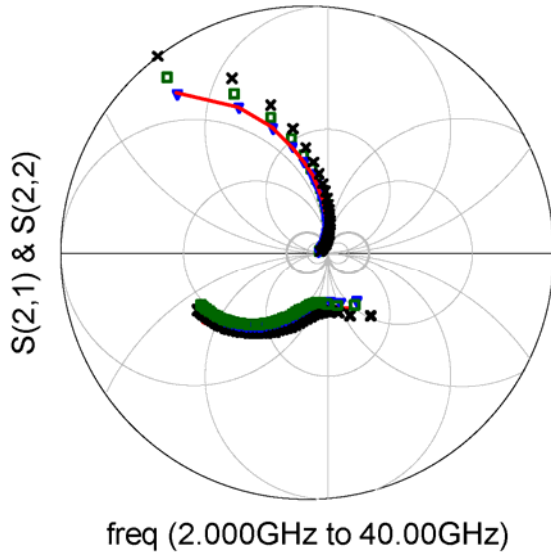


Fig.5 $S(2,1)$ and $S(2,2)*8$ parameters of a $0.25\mu\text{m}$ Triquint PHEMT biased at $V_{gs} = -0.55\text{V}$ $V_{ds} = 6.5\text{V}$. Measurements (solid line) versus predictions based on Backgating (squares), Empirical (triangles) and with the purely static DC IV characteristic (crosses) models.

For example the S_{21} and S_{22} parameters (more evidently affected by dispersion) predicted by means of the NDC model using the two different LF dispersive i/v models are shown in Fig.5 together with the results obtained by using only the purely DC I/V characteristics in the NDC model identification. In the latter case it is well evident the poor prediction capability due to lack of the low-frequency dispersion modelling. As can be seen the prediction capability of the microwave device model, also at high frequency, is affected by the i/v model used to take into account the dispersive effects.

In order to evaluate the nonlinear high-frequency prediction accuracy of the models, measurements of the third-order intermodulation product (interferer) to carrier ratio (I/C) were carried out at the frequency of 39.9GHz (two tone displacement: 10MHz; class-A operation: $I_b=60\text{mA}$, $V_{DS}=6.5\text{V}$). Simulation and measurement results are shown in Fig.6 as a function of the output power. As can be seen, the NDC model with embedded the backgating i/v model is in good agreement with measurements, despite the very low level of the IMD products required by the specific application. In the same figure, also the simulation

results obtained by using the new Empirical model are shown, in such a case, it is well evident the higher level of accuracy. Finally the poor prediction capability obtained making use of the purely static DC I/V characteristics are shown in the same figure.

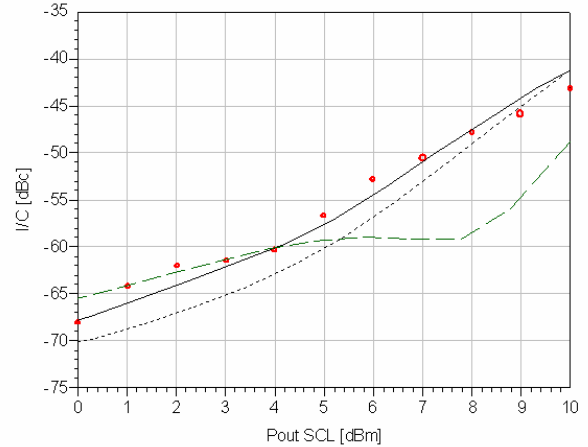


Fig.6 Third-order intermodulation product (Interferer) to Carrier ratio versus output power (Single Carrier Level) for the $0.25\mu\text{m}$ Triquint GaAs PHEMT at 39.9 GHz [Bias: $I_{d0} = 60\text{ mA}$, $V_{d0} = 6.5\text{ V}$, Load $\Gamma_L = (0.7\angle 168^\circ)$, Source $\Gamma_s = (0.871\angle -177^\circ)$]. Measurements (circles) are compared to predictions based on the NDC model [5] with embedded the Backgating (dot line), the Empirical (solid line) and the purely static I/V (dashed line) models.

IV. CONCLUSION

A new large-signal measurement setup has been exploited for the identification of two different models of low frequency dispersive effects in FETs. Validation of the two models at low frequencies under small and large signal conditions has been provided. Finally the impact of low frequency modelling on high frequency large-signal performances has been also shown.

ACKNOWLEDGMENT

The Authors wish to thank Francesco Scappaviva and Stefano Menghi for their contribution in the CAD simulations and device measurements.

REFERENCES

- [1] A.Raffo, A.Santarelli, P.A.Traverso, G.Vannini, F.Filicori, "On-wafer I/V measurement setup for the characterization of low-frequency dispersion in electron devices," in IEEE 63rd ARFTG Dig., Jun. 2004.
- [2] F.Filicori, G. Vannini, A. Santarelli, A.M. Sanchez, A. Tazon and Y. Newport, "Empirical modeling of low-frequency dispersive effects due to traps and thermal phenomena in III-V FET's," IEEE Trans. Microwave Theory and Techn., vol. 43, pp. 2972-2981, Dec. 1995.
- [3] Paper to be published.
- [4] A.Santarelli, G.Vannini, F.Filicori, P.Rinaldi "Backgating model including self-heating for low-frequency dispersive effects in III-V FETs," Electron. Lett., vol.34 no.20, pp.1974-1976, Oct. 1998.
- [5] Fabio Filicori, Alberto Santarelli, Pier Andrea Traverso, Giorgio Vannini, "Electron Device Model Based On Nonlinear Discrete Convolution For Large-Signal Circuit Analysis Using Commercial Cad Packages", Proc. of Gallium Arsenide Application Symposium, Oct. 1999, 225-230.